# Interactions between NADPH oxidase-related proton and electron currents in human eosinophils

T. E. DeCoursey, V. V. Cherny, A. G. DeCoursey, W. Xu* and L. L. Thomas*

*Department of Molecular Biophysics and Physiology and *Department of Immunology/Microbiology, Rush Presbyterian St Luke's Medical Center, Chicago, IL 60612, USA*

(Received 8 February 2001; accepted after revision 14 May 2001)

1. Proton and electron currents in human eosinophils were studied using the permeabilized-patch voltage-clamp technique, with an applied $NH_4^+$ gradient to control $pH_i$.

2. Voltage-gated proton channels in unstimulated human eosinophils studied with the permeabilized-patch approach had properties similar to those reported in whole-cell studies.

3. Superoxide anion ($O_2^-$) release assessed by cytochrome *c* reduction was compared in human eosinophils and neutrophils stimulated by phorbol myristate acetate (PMA). PMA-stimulated $O_2$ release was more transient and the maximum rate was three times greater in eosinophils.

4. In PMA-activated eosinophils, the $H^+$ current amplitude ($I_H$) at +60 mV increased 4.7-fold, activation was 4.0 times faster, deactivation (tail current decay) was 5.4 times slower, the $H^+$ conductance–voltage ($g_H$–$V$) relationship was shifted −43 mV, and diphenylene iodinium (DPI)-inhibitable inward current reflecting electron flow through NADPH oxidase was activated. The data reveal that PMA activates the $H^+$ efflux during the respiratory burst by modulating the properties of $H^+$ channels, not simply as a result of NADPH oxidase activity.

5. The electrophysiological response of eosinophils to PMA resembled that reported in human neutrophils, but PMA activated larger proton and electron currents in eosinophils and the response was more transient.

6. $ZnCl_2$ slowed the activation of $H^+$ currents and shifted the $g_H$–$V$ relationship to more positive voltages. These effects occurred at similar $ZnCl_2$ concentrations in eosinophils before and after PMA stimulation. These data are compatible with the existence of a single type of $H^+$ channel in eosinophils that is modulated during the respiratory burst.

The NADPH oxidase enzyme complex is a critically important component of the host defence system against bacterial invaders. In resting phagocytes NADPH oxidase is inactive, with its several protein components partitioned between the cytosolic and membrane compartments (Babior, 1999). The active enzyme is assembled in the membranes of phagocytes upon cell activation by phagocytic stimuli such as opsonized bacteria or by soluble stimuli such as chemotactic peptides and the artificial stimulus phorbol myristate acetate (PMA). The active NADPH oxidase complex generates the superoxide anion ($O_2^-$) and other reactive oxygen intermediates that are toxic to micro-organisms. The importance of these reactions is evident in chronic granulomatous disease, in which the absence of a functioning NADPH oxidase is manifested as a lethal susceptibility to recurrent bacterial infection if left untreated (Babior, 1999).

NADPH oxidase is electrogenic, transporting electrons out of the cell in order to reduce $O_2$ to $O_2^-$, and compensatory electrogenic proton efflux is activated during the respiratory burst (Henderson *et al.* 1987, 1988*a*,*b*; Nanda & Grinstein, 1991). Henderson *et al.* (1987, 1988*a*,*b*) postulated that this $H^+$ efflux was mediated by voltage-gated proton channels. In support of this hypothesis, voltage-gated proton currents have been found in every phagocyte or related cell line that has been studied (Eder & DeCoursey, 2001), but many questions remain. Although NADPH oxidase-associated electron flux and $H^+$ efflux are both activated by PMA, a potent agonist for the respiratory burst, it is not clear whether the $H^+$ conductance ($g_H$) is activated independently by PMA or indirectly as a consequence of the oxidase functioning. Both the decrease in $pH_i$ and the depolarization of the membrane potential that tend to occur when the oxidase functions can activate voltage-

gated proton channels. A role for diffusible intracellular second messengers in the activation of both electron and proton currents in human neutrophils is suggested by the observation that PMA is ineffective in whole-cell studies but activates both electron and proton currents in the permeabilized-patch configuration (DeCoursey *et al.* 2000). The oxidase inhibitor diphenylene iodinium (DPI) inhibited the electron currents, which reflect NADPH oxidase activity, but not the increased $H^+$ current amplitude in neutrophils, indicating dissociation between the operation of these two conductances. However, the PMA-induced slowing of the closing rate of $H^+$ channels was reversed by DPI, suggesting that some functional link exists between NADPH oxidase and voltage-gated proton channels (DeCoursey *et al.* 2000).

Like neutrophils, eosinophils play an important role in host defence and are also implicated in the pathogenesis of a number of disorders, including most notably asthma and other allergic inflammatory disorders (Rothenberg, 1998; Gleich, 2000). The composition of the NADPH oxidase system in eosinophils is similar to that in neutrophils and other phagocytes (Someya *et al.* 1997; Giembycz & Lindsay, 1999), and generation by this enzyme of $O_2^-$ and other oxygen radicals contributes to both the host defence and pathogenic activities of eosinophils (Wu *et al.* 2000). Indeed, eosinophils exhibit a particularly vigorous respiratory burst compared with neutrophils and other phagocytes (DeChatelet *et al.* 1977; Yamashita *et al.* 1985; Shult *et al.* 1985; Petreccia *et al.* 1987; Yagisawa *et al.* 1996; Someya *et al.* 1997), with consequently larger electron currents (Schrenzel *et al.* 1998; DeCoursey *et al.* 2000). Their vigorous respiratory burst and the existence of techniques that allow their ready isolation (Hansel *et al.* 1991) make the human eosinophil an attractive cell for the study of NADPH oxidase function.

It was proposed recently that eosinophils have two distinct varieties of voltage-gated proton channels, one that is present in resting cells, and another with different properties that is activated during the respiratory burst (Bánfi *et al.* 1999). We named these channels type p and type x respectively, for '*p*hagocyte' and 'o*x*idase' (Eder & DeCoursey, 2001). However, several types of evidence suggest that there is a single type of voltage-gated proton channel in neutrophils, whose properties are modulated strongly when NADPH oxidase is activated by PMA (DeCoursey *et al.* 2000). The voltage-gated proton conductance that is activated during the respiratory burst in human eosinophils resembles that activated in human neutrophils (DeCoursey *et al.* 2000), and the data are consistent with the idea that a single population of $H^+$ channels exists in human eosinophils or neutrophils.

A preliminary account of this work has been published (Cherny *et al.* 2001*a*).

# METHODS

### Eosinophil and neutrophil isolation

Venous blood was drawn from healthy adult volunteers under informed consent according to procedures approved by our Institutional Review Board and in accordance with Federal regulations. Neutrophils were isolated by density gradient centrifugation as described previously (Haskell *et al.* 1995) with one modification. In the two cycles of hypotonic lysis performed for removal of the red blood cells, isotonicity was restored by the addition of 2× concentrated Hanks' balanced salt solution (HBSS; cat. no. 14185, Gibco, Grand Island, NY, USA) (without $Ca^{2+}$ or $Mg^{2+}$) containing 5 mM Hepes, and adjusted to pH 7.4. An aliquot of the neutrophil preparation was held on ice, and eosinophils were isolated from the neutrophil preparation by negative selection using anti-CD16 immunomagnetic beads (Hansel *et al.* 1991) as described by the manufacturer (Miltenyi Biotec Inc., Auburn, CA, USA). The eosinophils or neutrophils were suspended in Hepes (10 mM)-buffered HBSS (with $Ca^{2+}$ and $Mg^{2+}$, Gibco cat. no. 14065), adjusted to pH 7.4, containing 1 mg $ml^{-1}$ human serum albumin (Hepes–HBSS–HSA buffer). Eosinophil purity was routinely greater than 98% as determined by counting Wright-stained cytospin preparations. Neutrophil purity was routinely 95% or greater. Cells from at least 14 different donors were used in this study.

### Superoxide anion production

Superoxide anion ($O_2^-$) production was measured essentially as described elsewhere (Horie & Kita, 1994). Briefly, eosinophils or neutrophils (each at $2.5 \times 10^5$ cells $ml^{-1}$) were incubated with 8 nM PMA in Hepes–HBSS–HSA buffer containing 50 $\mu$M cytochrome *c* for 45 min at 37 °C. Incubations were performed in a flat-bottomed 96-well tissue culture plate (Costar, Acton, MA, USA) in a Ceres UV900HDi microplate reader (Bio-Tek Instruments, Inc., Winooski, VT, USA), and absorbance at 550 nm was recorded at 5 min intervals. Tissue culture wells were precoated with human serum albumin (Horie & Kita, 1994). Total incubation volume was 0.2 ml. Production of $O_2^-$ was calculated as described previously (Horie & Kita, 1994). Results are expressed in nanomoles $O_2^-$ per $10^5$ cells after subtraction of spontaneous production, which was measured in the absence of PMA stimulus.

### Electrophysiology

We studied freshly isolated eosinophils and eosinophils incubated overnight at 37 °C in RPMI 1640 medium containing 25 mM Hepes and L-glutamine (Gibco), supplemented with 10% fetal bovine serum (Bio-Whittaker, Walkersville, MD, USA), 100 units $ml^{-1}$ penicillin, 100 $\mu$g $ml^{-1}$ streptomycin (Sigma), and 1 ng $ml^{-1}$ recombinant human GM-CSF (R & D Systems, Inc., Minneapolis, MN, USA). No difference between the properties or responses of freshly isolated and incubated eosinophils was detected.

For permeabilized-patch recording, the pipette and bath solutions usually contained 50 mM $NH_4^+$ in the form of 25 mM $(NH_4)_2SO_4$, 2 mM $MgCl_2$, 5 mM Bes or Pipes buffer, 1 mM EGTA, and were adjusted to pH 7.0 with TMAOH. We added ~500 $\mu$g $ml^{-1}$ solubilized amphotericin B (~45% purity) (Sigma) to the pipette solution, after first dipping the tip in amphotericin-free solution.

Micropipettes were pulled using a Flaming-Brown automatic pipette puller (Sutter Instruments, San Rafael, CA, USA) from 7052 glass (Garner Glass Co., Claremont, CA, USA), coated with Sylgard 184 (Dow Corning Corp., Midland, MI, USA), and heat polished to a tip resistance ranging typically between 3 and 10 MΩ. Electrical contact with the pipette solution was achieved by a thin sintered Ag–AgCl pellet (In Vivo Metric Systems, Healdsburg, CA, USA) attached to a Teflon-encased silver wire, or simply a chlorided silver wire. A

reference electrode made from a Ag–AgCl pellet was connected to the bath through an agar bridge made with Ringer solution (containing (mM): 160 NaCl, 4.5 KCl, 2 $CaCl_2$, 1 $MgCl_2$, 5 Hepes, adjusted to pH 7.4). The current signal from the patch clamp (EPC-7 from List Electronic, Darmstadt, Germany, or Axopatch 200B from Axon Instruments, Foster City, CA, USA) was recorded and analysed using an Indec Laboratory data acquisition and display system (Indec Corporation, Sunnyvale, CA, USA) or pCLAMP software supplemented by Microsoft Excel and SigmaPlot (SPSS Inc., Chicago, IL, USA). Seals were formed with Ringer solution in the bath, and the potential zeroed after the pipette was in contact with the cell. For the experimental set-up where most measurements were done, the bath temperature was kept at 20–21 °C by Peltier devices and monitored by a resistance temperature detector (RTD) element (Omega Scientific, Stamford, CT, USA) in the bath. For the other experimental set-ups, data were collected at room temperature (20–25 °C).

### Heterogeneous responses to stimulation and possible effects of adherence

There was variability in the behaviour of unstimulated eosinophils and in their response to PMA. Within the first ~10 min of establishing a seal, the proton current ($I_H$) tended to increase and often the reversal potential ($V_{rev}$) shifted from a positive value to near 0 mV. $I_H$ would be expected to increase over time as the amphotericin in the pipette inserts into the membrane and establishes control over the membrane potential. Most measurements were done with a symmetrical $NH_4^+$ gradient, nominally setting $pH_i$ to 7.0, which is lower than is likely to occur in an untreated eosinophil. $I_H$ would tend to increase as $pH_i$ decreases. We started to make measurements after the $H^+$ currents exhibited stable behaviour.

In the absence of any added stimulus some cells exhibited signs of 'activation': slow tail current decay, activation at voltages near or negative to the proton equilibrium potential ($E_H$), and in some cases inward current (presumed electron current) at a holding potential ($V_h$) of −60 mV. These signs were present immediately, developed over time, or disappeared over time. Cells displaying spontaneous activation responded to DPI with speeding of the tail current time constant ($\tau_{tail}$) and block of inward electron current at −60 mV (Cherny *et al.* 2001*b*, Fig. 2), confirming that the spontaneously active state included both NADPH oxidase activity and the attendant changes in $H^+$ current properties associated with PMA activation. As was found in neutrophils (DeCoursey *et al.* 2000), DPI had no effect on non-activated eosinophils, $H^+$ currents or the leak current.

In early studies, we noticed that eosinophils that were allowed to settle onto the glass chamber rapidly became attached and began to spread. Our impression was that these adherent cells were more likely than non-adherent cells to appear 'activated' (according to the criteria listed in the previous paragraph) as soon as recording had begun. Because they seemed less predisposed to adhere to albumin-coated glass, eosinophils were placed above coverslip fragments precoated by incubation with 20% bovine serum albumin (Sigma). Although this precaution appeared to reduce spontaneous activation, some cells still displayed signs of activation. In many cells, these signs disappeared within a few minutes, after which the cell was capable of responding to a challenge with PMA.

### Bath solution changes

Solutions and physiologically active substances were applied by flushing the entire bath solution (~400 μl volume) with ~10 bath volumes, which took ~10–20 s. The time of a bath change was taken as roughly the time the first volume replacement occurred. We did not perfuse the chamber continuously. As a control for mechanically induced responses, the bath solution was usually first replaced with an identical solution before adding a test solution. Changing the bath solution transiently increases $H^+$ currents due to a small increase in temperature. Due to the strong temperature sensitivity of the $H^+$ current (Kuno *et al.* 1997; DeCoursey & Cherny, 1998), even an ~1 °C change has a definite effect.

### Conventions

Currents and voltages are presented in the normal sense: upward currents represent positive charge flowing outward through the membrane, and potentials are expressed relative to the potential of the original bath solution which is defined as 0 mV. Current records are presented without correction for leak current or liquid junction potentials.

### Data analysis

The time constant of $H^+$ current activation ($\tau_{act}$) was obtained by fitting the current record by eye with a single exponential after a brief delay (DeCoursey & Cherny, 1995):

$$I(t) = (I_0 - I_\infty)\exp(-(t - t_{delay})/\tau_{act}), \quad (1)$$

where $I_0$ is the initial amplitude of the current after the voltage step, $I_\infty$ is the steady-state current amplitude, $t$ is the time after the voltage step, and $t_{delay}$ is the delay. The $H^+$ current amplitude is $(I_0 - I_\infty)$. No other time-dependent conductances were observed consistently under the ionic conditions employed. Tail current time constants ($\tau_{tail}$) were obtained by fitting tail currents to a single exponential:

$$I(t) = I_0\exp((-t/\tau_{tail}) + I_\infty), \quad (2)$$

where $I_0$ is the amplitude of the decaying part of the tail current.

## RESULTS

### Properties of voltage-gated proton currents in unstimulated eosinophils in the permeabilized patch configuration

Eosinophils were studied using the permeabilized-patch approach in order to preserve intracellular second messenger pathways. We established an $NH_4^+$ gradient in order to 'clamp' $pH_i$ (Grinstein *et al.* 1994; DeCoursey *et al.* 2000). In most experiments the $NH_4^+$ gradient was symmetrical (50 mM $NH_4^+$ in bath and pipette solutions), which kept the $pH_i$ near $pH_o$ (7.0 unless otherwise stated). Under these conditions, most human eosinophils exhibited robust voltage-gated proton currents, as illustrated in Fig. 1*A*. The average $H^+$ current measured at the end of an 8 s pulse to +80 mV was 48 ± 31 pA (mean ± S.D.) in a sample of 16 consecutively studied eosinophils. The $H^+$ selectivity of these currents was confirmed by measuring the tail current reversal potential ($V_{rev}$) as illustrated in Fig. 1*B*. In this experiment, the tail currents reversed near 0 mV, consistent with the symmetrical $NH_4^+$ gradient. When $pH_i$ was varied indirectly by changing the $NH_4^+$ concentration in the bath solution $V_{rev}$ changed in reasonable agreement with the Nernst potential for $NH_4^+$, which ideally establishes an identical $H^+$ gradient. In one to four measurements at each $[NH_4^+]_o$ in three cells studied with 50 mM $NH_4^+$ in the pipette solution, $V_{rev}$

averaged −32 mV at 15 mM $NH_4^+$ ($E_H = -30$ mV), −44 mV at 9 mM $NH_4^+$ ($E_H = -43$ mV), −70 mV at 3 mM $NH_4^+$ ($E_H = -71$ mV), and −82 mV at 1 mM $NH_4^+$ ($E_H = -99$ mV). Thus, the time-dependent currents are $H^+$ selective and the applied $NH_4^+$ gradient is adequate to establish $pH_i$, as was previously demonstrated using this approach in human neutrophils (DeCoursey *et al.* 2000).

### Gating kinetics

The kinetics of $H^+$ current activation during a depolarizing pulse was quantified by fitting a single exponential after a delay. During large depolarizations the $H^+$ current in some cells continued to rise progressively at a slower rate. These currents could be fitted arbitrarily with an exponential plus a linearly rising component. We adopted the single exponential approach rather than introducing a more complex function for three reasons: (1) it is simple; (2) we have used it previously in a number of cell types; and (3) as a result of the high $H^+$ current density in eosinophils, diffusion artifacts may alter the apparent kinetics.

The activation time constant ($\tau_{act}$) obtained in this way is plotted in Fig. 1*C* (○). Activation of $H^+$ current was faster at more positive potentials, but with modest voltage dependence, with $\tau_{act}$ changing e-fold in 59 mV. The time constant of deactivation of the $H^+$ current ($\tau_{tail}$) was obtained by fitting tail currents like those illustrated in Fig. 1*B* with a single exponential. A single exponential provided a good fit over the entire voltage range negative to the threshold for activating the $H^+$ conductance ($g_H$). The voltage dependence of deactivation was almost twice as steep as that of activation, with $\tau_{tail}$ changing e-fold in 32 mV (Fig. 1*C*, □).

### Effects of PMA on $H^+$ currents

Although PMA has no effect on $H^+$ currents in phagocytes studied in whole-cell configuration, profound effects are observed in permeabilized-patch recording conditions (DeCoursey *et al.* 2000). Figure 2*A* and *B* illustrates families of voltage-gated proton currents recorded in the same eosinophil before and after addition of PMA. After PMA stimulation, the $H^+$ current ($I_H$) is larger and the $g_H$ was activated at substantially more negative voltages. The NADPH oxidase inhibitor DPI had little immediate effect on $H^+$ currents in PMA-stimulated cells (Fig. 2*C*), except that it accelerated tail current decay. $I_H$ was somewhat larger after DPI treatment in this cell, but this effect was not always seen.

Activation of voltage-gated proton channels in unstimulated eosinophils occurred at potentials more positive than +20 mV (Fig. 2*D*). After PMA treatment, the $g_H - V$ relationship shifted toward substantially more negative voltages. We quantified this shift by estimating the threshold voltage at which time-dependent currents were first elicited ($V_{threshold}$), or after which distinct tail currents were seen upon repolarization to −60 mV. The average shift in $V_{threshold}$ produced by PMA in eosinophils by these criteria was $-42.6 \pm 1.8$ mV (mean ± S.E.M., $n = 23$). The addition of DPI did not change $V_{threshold}$ much, although a slight depolarizing shift was sometimes evident. Often $I_H$ increased somewhat, as in Fig. 2*D*, but it is not clear whether this was a genuine effect of DPI or simply the continuation of progressive enhancement by PMA. Long after PMA exposure in some cells there was a return toward control values of all parameters. In these cells, the $g_H - V$ relationship gradually shifted toward

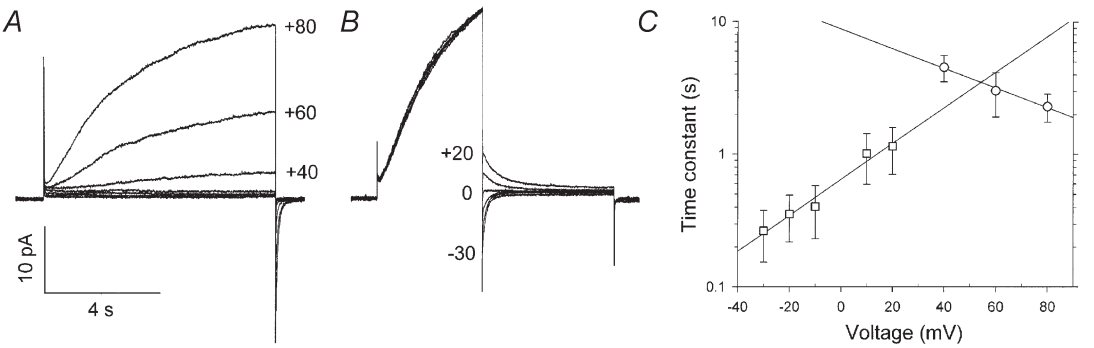


**Figure 1. Properties of voltage-gated proton currents in unstimulated human eosinophils studied using the permeabilized patch technique**

*A*, a family of currents during 8 s voltage pulses (at 30 s intervals) from −40 mV through +80 mV in 20 mV increments from $V_h = -60$ mV. *B*, tail currents measured in the same cell. A 4 s prepulse to +80 mV opened $H^+$ channels, then the potential was stepped to −30 mV through +20 mV in 10 mV increments. $V_{rev}$ is close to 0 mV, as expected for a symmetrical pH gradient (50 mM $NH_4^+$ in pipette and bath solutions, pH 7.0). Low-pass filtered at 100 Hz. *C*, mean ± S.D. time constants of activation, $\tau_{act}$ (○), and deactivation (tail current decay), $\tau_{tail}$ (□), are plotted ($n = 10$–12 cells), with lines showing linear regression slopes of 59 mV per e-fold change in voltage and 32 mV per e-fold change in voltage, respectively. The fitted lines show the following relationships: $\tau_{act} = 8.80\exp(V/-58.7)$, and $\tau_{tail} = 0.646\exp(V/32.2)$, where $V$ is the voltage in millivolts and the time constants are in seconds.

more positive voltages, $I_H$ became smaller, $\tau_{act}$ became slower, and $\tau_{tail}$ became faster.

Because the $g_H - V$ relationship shifted toward substantially more negative voltages after PMA treatment, the threshold often occurred at potentials more negative than $V_{rev}$, which resulted in the activation of inward $H^+$ currents. Inward $H^+$ currents are not normally observed in cells studied in whole-cell recording conditions (Eder & DeCoursey, 2001), but occur in eosinophils under conditions that activate NADPH oxidase (Bánfi *et al.* 1999). These currents are small because the driving force near $V_{rev}$ is small; however, they can be seen at high gain (data not shown), and can be confirmed by examination of the tail currents upon repolarization to −60 mV.

The effect of PMA on $\tau_{act}$ is shown in Fig. 2*E*. The average values of $\tau_{act}$ measured at several voltages before (○) and after PMA (■) are plotted. To a first approximation, the activation rate increased uniformly at all voltages. Also plotted is the average $\tau_{act}$ in cells that eventually reverted to control-like behaviour (△).

### Shifts of $V_{rev}$

Because NADPH oxidase generates intracellular protons, its activation will tend to lower $pH_i$. In our experiments, this tendency is opposed by the applied $NH_4^+$ gradient, but the additional acid load on this system may still result in a lower $pH_i$. Indeed, $V_{rev}$ measured after PMA treatment tended to be more negative than in the same cells before PMA. The average change in $V_{rev}$ in 16 cells measured before and after exposure to 30–60 nM PMA was −5.8 ± 1.5 mV (mean ± S.E.M.), indicating that slight cytoplasmic acidification (~0.1 pH unit) did occur in spite of the $NH_4^+$ gradient. Cytoplasmic acidification due to

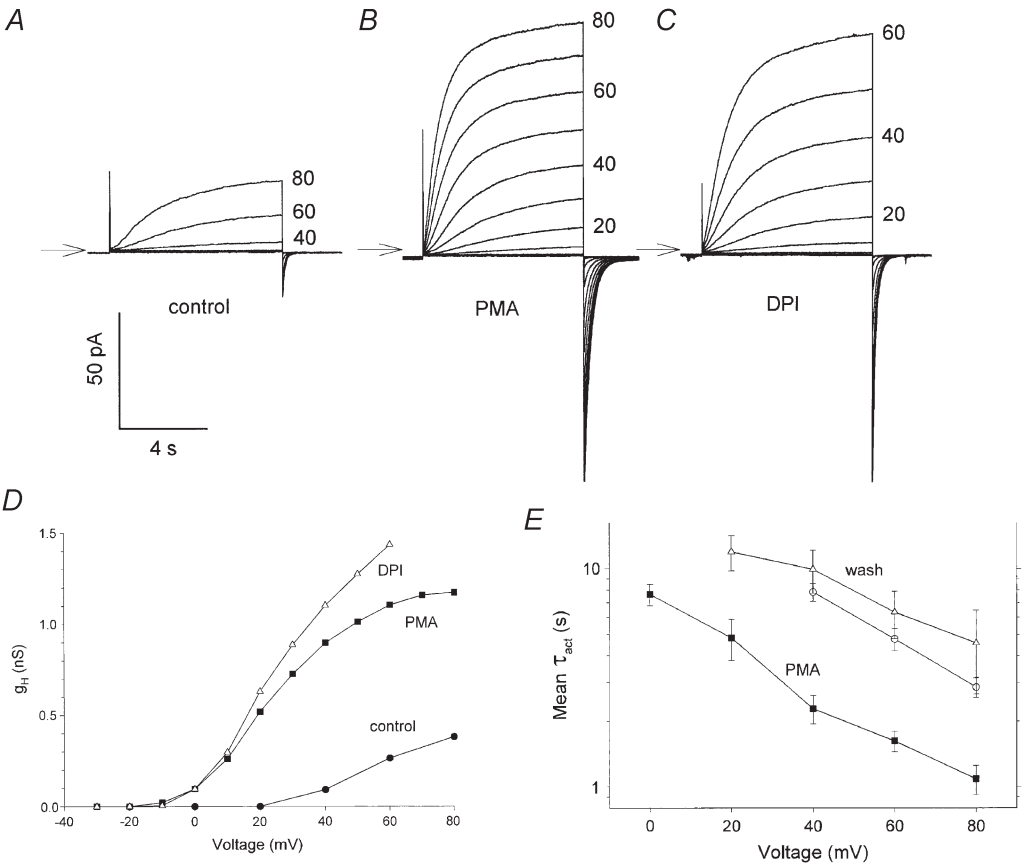


**Figure 2. Effects of PMA and DPI on $H^+$ current properties**

*A*, currents recorded in an untreated eosinophil during depolarizing pulses from $V_h = -60$ mV to −40 mV through +80 mV in 20 mV increments are superimposed. *B*, currents in the same cell after addition of 30 nM PMA. Pulses were applied in 10 mV increments. *C*, currents in the same cell after addition of 3 μM DPI (and washout of PMA). The arrows indicate the level of zero current. *D*, chord conductance–voltage relationships in the same eosinophil as in *A*–*C*, before (●) and after PMA (■), and after treatment with DPI (△). Conductances were calculated from the net $H^+$ current (defined as the time-dependent current) measured at the end of 8 s pulses like those in *A*, using $V_{rev}$ measured in each solution (+4 mV control, −2.4 mV in PMA, and −4 mV in DPI). *E*, voltage dependence of $\tau_{act}$ in eosinophils before stimulation (○), after PMA activation (■), and after washout and recovery (△). Means ± S.E.M. are plotted for $n = 13$–14, 5–9, or 2–4 cells, respectively. In most cells DPI was added after PMA; only cells in which $H^+$ current parameters returned to near normal (e.g. the cell in Fig. 5) are included in the 'wash' group.

the activity of NADPH oxidase should be reversed by DPI. In seven cells in which $V_{rev}$ was measured after PMA and again after DPI, the average change in $V_{rev}$ was +3.0 ± 0.8 mV.

### Superoxide anion release by eosinophils induced by PMA

Voltage-gated proton channels are believed to play a role during the respiratory burst in eosinophils and other phagocytes (Henderson & Chappell, 1996; DeCoursey & Grinstein, 1999). We therefore examined superoxide production in response to PMA stimulation in eosinophils. Figure 3*A* shows the time course of PMA-stimulated superoxide production by neutrophils (□) and eosinophils (●) from four donors. Consistent with previous studies (DeChatelet *et al.* 1977; Yamashita *et al.* 1985; Shult *et al.* 1985; Petreccia *et al.* 1987; Freiburghaus *et al.* 1991; Yagisawa *et al.* 1996; Someya *et al.* 1997), the respiratory burst was larger and faster in eosinophils than in neutrophils. The difference in the time course is more apparent when the rate of $O_2^-$ release is plotted, as in Fig. 3*B*. In both cell types, the peak $O_2^-$ production occurred 5–10 min after PMA addition. In eosinophils, the respiratory burst was transient, with no $O_2^-$ released after 25 min. In neutrophils release persisted longer and was still ~40 % the maximal rate 40 min after PMA stimulation. The peak rate in eosinophils was 3.2 times greater than in neutrophils.

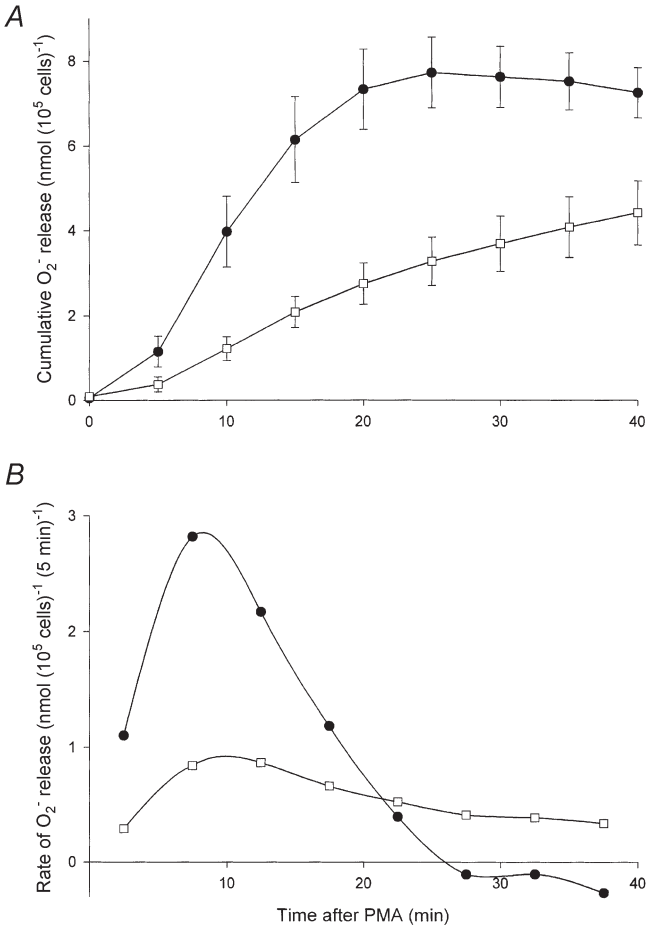


**Figure 3. Time course of PMA-stimulated $O_2^-$ release from human eosinophils and human neutrophils**

*A*, comparison of net cumulative $O_2^-$ release from human eosinophils (●) and human neutrophils (□). Means ± S.E.M. are plotted for determinations of each cell type from the same four individuals. At time 0 the cells were stimulated with 8 nM PMA. *B*, rate of $O_2^-$ release from human eosinophils (●) and human neutrophils (□). The data in *A* are replotted as the increment of $O_2^-$ released in each 5 min interval. The points are positioned in the middle of their time bins, and the spline curve through the points is arbitrary.

### Time course of PMA effects

Figure 4*A* illustrates the time course of PMA effects on proton and electron currents in an eosinophil. Pulses were applied from $V_h = -60$ mV to a test potential of +60 mV at 30 s intervals. Characteristically, $I_H$ increased after a delay. In Fig. 4*A*, no effect was observed 30 s after addition of 30 nM PMA, and the maximal rate of change occurred 1–2 min after stimulation. In addition to increasing $I_H$ substantially, PMA stimulation caused the $H^+$ current activation time course to become faster (smaller $\tau_{act}$). Finally, the rate of tail current decay (the rate that $H^+$ channels close upon repolarization to −60 mV) became slower ($\tau_{tail}$ increased).

In addition to its effects on the $H^+$ conductance, PMA usually activated an inward current in eosinophils. The progressive increase in the inward current at −60 mV after PMA stimulation is evident in Fig. 4*A* and also can be seen in Fig. 2 (note arrows indicating zero current). As shown in Fig. 4*B* (+), this current was inhibited by DPI, an inhibitor of NADPH oxidase (Robertson *et al.* 1990). The inward current therefore reflects the efflux of electrons across the membrane mediated by NADPH oxidase and is termed electron current ($I_e$). The $I_e$ amplitude was on average −6 pA (Table 1), which is several times larger than in neutrophils studied under similar conditions (DeCoursey *et al.* 2000). In contrast to the $H^+$ current, which can be observed only by applying a depolarizing voltage pulse to open voltage-gated proton channels, $I_e$ is not voltage gated. Thus, it can be observed at −60 mV where there is no $H^+$ current. This lack of voltage- and time-dependent gating of $I_e$ allows clear separation from $I_H$ and enables both to be monitored in the same cell at essentially the same time.

Figure 4*B* shows the time course of the changes in $H^+$ currents produced by PMA. Shortly after addition of PMA, activation (▲) of $H^+$ currents became faster, the $I_H$ amplitude (●) increased, and deactivation (□) of $H^+$ currents became slower. Distinct inward electron current ($I_e$, +) appeared after a delay of 1–2 min. Addition of DPI turned off most of the PMA-induced inward current, supporting its origin as electron flux through the NADPH oxidase complex. DPI also largely reversed the slowing of

**Table 1. Magnitude and time course of effects of PMA in eosinophils**

| | $\tau_{act}$ (PMA/control) | $\tau_{tail}$ (PMA/control) | $I_H$ (PMA/control) | $I_e$ (pA) |
|---|---|---|---|---|
| Eosinophils | 0.24 ± 0.09 (12) | 5.4 ± 3.4 (14) | 4.7 ± 2.8 (12) | −6.0 ± 2.8 (23) |
| Neutrophils | 0.27 | 5.5 | 3.3 | −2.3 |
| $t_{1/2}$ eosinophils (min) | 1.0 ± 0.6 (12) | 1.6 ± 0.7 (14)* | 2.0 ± 1.5 (12) | 2.5 ± 2.1 (17) |
| $t_{1/2}$ neutrophils (min) | < 1 | 4.3 | 3.4 | 3.0 |

The first row gives the average ratio of each parameter (except $I_e$) measured after treatment with 30–60 nM PMA to its value before treatment. Usually $I_H$ and $\tau_{act}$ were measured during pulses to +40 or +60 mV, and $\tau_{tail}$ and $I_e$ at −60 mV. $I_e$ is taken as the average peak increase in inward current after PMA. Mean ± S.D. is given for ($n$) observations. Neutrophil values are taken from DeCoursey *et al.* (2000) for human neutrophils stimulated with PMA under identical conditions. The $t_{1/2}$ value is the time required for the change to reach half-completion. * Significantly faster for eosinophils than neutrophils ($P < 0.01$ by Student's two-tailed $t$ test).

$\tau_{tail}$ produced by PMA, but DPI did not reverse the enhanced $I_H$ or the faster $\tau_{act}$. These effects of PMA are very similar to those reported previously in human neutrophils (DeCoursey *et al.* 2000). It should be emphasized, however, that there was considerable heterogeneity in the kinetics and magnitude of eosinophil responses to PMA. A remarkable result seen in this and most other experiments is that the time courses of changes in $\tau_{tail}$ and $I_e$ paralleled each other.

The time courses of the changes in the electrophysiological parameters are summarized in Table 1. Although the effects are quite similar to those described recently in

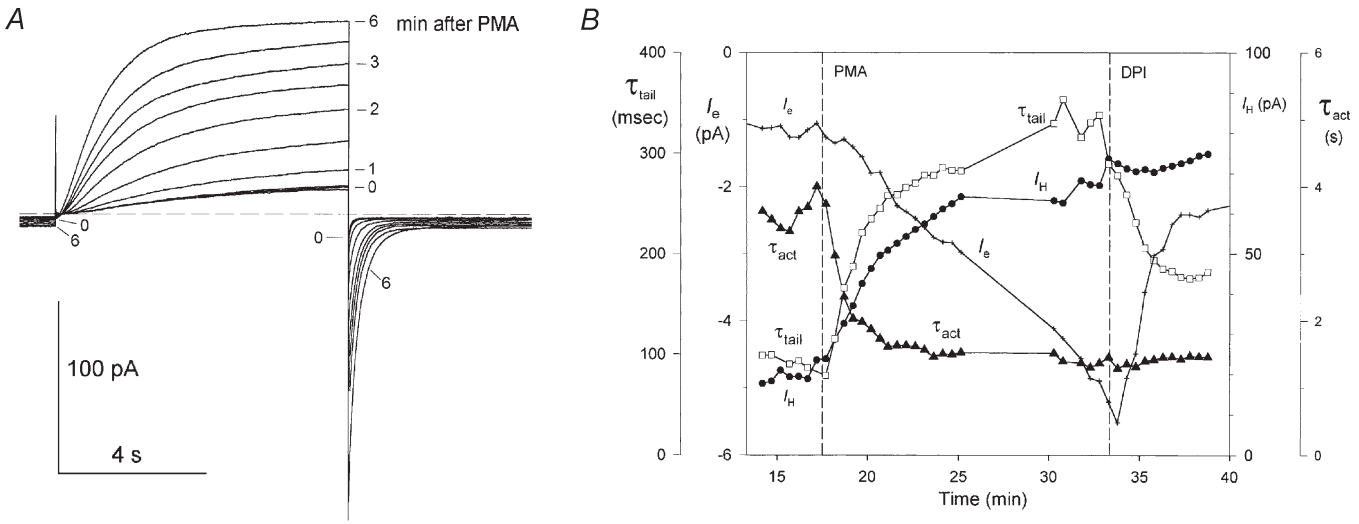


**Figure 4. Time dependence of the electrophysiological effects of PMA on human eosinophils in the permeabilized-patch configuration**

*A*, current records during test pulses to +60 mV from a holding potential of −60 mV are superimposed. The dashed line shows the zero current level. Two control currents (labeled '0') were recorded before and after a bath change to control for possible flow artifacts. After application of 30 nM PMA test pulses were applied every 30 s; the first 7 are shown here. The first current recorded after PMA addition is superimposed on the control currents. $I_H$ increased noticeably 1 min after PMA addition and increased progressively over the next several minutes. The largest current illustrates a quasi-steady-state reached ~6 min after PMA addition. The inward current at −60 mV (electron current) increased progressively after PMA addition, with the first and last record labelled according to the time after PMA addition (0 and 6 min). The tail currents increased in amplitude and became progressively slower. Low-pass filter 100 Hz. *B*, the changes in various parameters during exposure of another eosinophil to PMA and then DPI are plotted. The abscissae indicate roughly the time elapsed after establishing permeabilized patch recording. The dashed vertical lines indicate the time the bath solution was changed to introduce PMA or DPI, as indicated. $H^+$ current parameters are $I_H$ (●), $\tau_{tail}$ (□), and $\tau_{act}$ (▲). The total holding current measured at −60 mV is labelled $I_e$ (+) in the figure, because it gives information about the electron current – the actual net $I_e$ is the additional inward current beyond baseline that was induced by PMA.

human neutrophils studied under nearly identical conditions (DeCoursey *et al.* 2000), the response of eosinophils was slightly faster. As in neutrophils, the most rapid response was an increase in the rate of $H^+$ current activation. In Fig. 4*B*, $\tau_{act}$ was near its steady-state value before much $I_e$ had turned on.

### Spontaneous reversal of PMA effects

The PMA responses just described occurred in most eosinophils (42/51 or 82%). The changes in all four parameters, however, reversed spontaneously, at least to some extent, in about half the cells that survived at least 20 min after PMA treatment. Figure 5 illustrates one such cell. PMA had its usual effects on $H^+$ and electron currents, but before DPI was added, $I_e$ had almost entirely disappeared. In parallel, the profoundly slowed $\tau_{tail}$ returned to near its original value. It is noteworthy that in this cell in which $\tau_{tail}$ had spontaneously recovered almost completely, addition of DPI had little effect and did not decrease $\tau_{tail}$ beyond its original value. In contrast, in Fig. 4*B* DPI accelerated $\tau_{tail}$. Evidently, DPI reverses the slowing of $\tau_{tail}$ induced by PMA, but this effect is not mediated by a direct pharmacological action on $H^+$ channels. In other cells in which $I_e$ turned off spontaneously, the PMA-induced slowing of $\tau_{tail}$ usually reversed in parallel. In the experiment in Fig. 5, the $I_H$ amplitude and $\tau_{act}$ returned to near their original values after DPI was added, but it is not clear whether the addition of DPI was responsible for this reversal. In other experiments, such as in Fig. 4*B*, DPI did not reverse these two parameters. In those cells in which the enhanced $I_H$ and the faster $\tau_{act}$ returned toward control values, this recovery seemed to occur independently of the presence or absence of DPI.

As in the example in Fig. 5, the electron currents stimulated by PMA in many eosinophils were noticeably more transient than in neutrophils. Because electron current is not distinguishable from non-specific leak current unless it is shown to be inhibited by DPI, the entire time course of the response cannot be determined unambiguously. However, in a number of eosinophils, presumed $I_e$ appeared within a few minutes of PMA stimulation, and then disappeared spontaneously within 5–10 min. We believe that the inward current activated by PMA in the eosinophil shown in Fig. 5 was $I_e$, because it occurred in synchrony with the changes in $H^+$ currents that occurred during the PMA response. By contrast, the $I_e$ in neutrophils declined spontaneously over time only infrequently (DeCoursey *et al.* 2000). We cannot absolutely rule out the possibility that in some cells $H^+$ current parameters 'recovered' due to spontaneous patch rupture resulting in whole-cell configuration. However, the gradual time course of recovery and the survival of the cell in Fig. 5 with no increase in leak current suggests that spontaneous transition to whole-cell configuration in this cell is unlikely.

In Fig. 5, PMA was added for a second time after the electrophysiological parameters had returned to near their initial (unstimulated) values. There was no response. In other cells, repeated application of PMA sometimes produced a response, but the response was usually weaker than the initial response. During some secondary PMA exposures $I_e$ was activated and $I_H$ increased, but the changes in gating kinetics of $H^+$ currents were seen less often. We suspect that the durations of PMA and DPI exposures as well as the extent to which various parameters had returned toward normal influenced whether a secondary response occurred. It is noteworthy

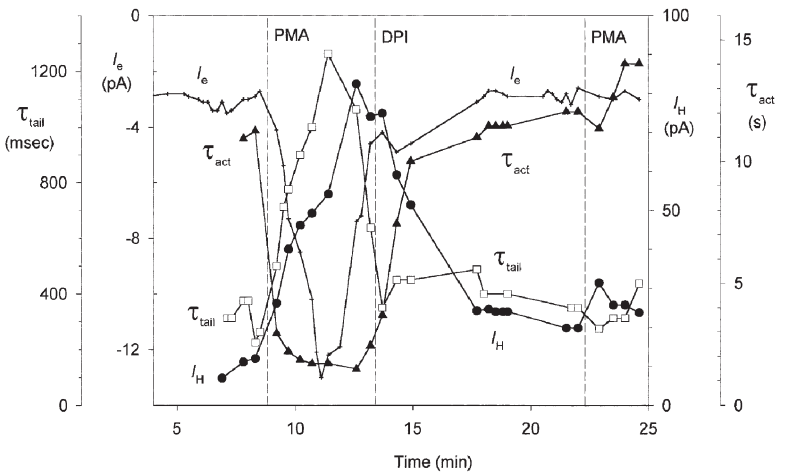


**Figure 5. An eosinophil exhibiting a transient response to PMA**

Time course of electrophysiological changes produced by PMA in an eosinophil, with the same symbol definitions as in Fig. 4*B*. $I_e$ (+) peaked ~3 min after PMA addition and then spontaneously turned off almost completely. Intriguingly, the slowing of $\tau_{tail}$ (□) peaked and reversed with a time course that is a mirror-image of the time course of $I_e$. Although $I_H$ (●) and $\tau_{act}$ (▲) also reversed almost completely after addition of DPI, this was probably not a direct effect of DPI, because DPI did not affect these parameters in the experiment shown in Fig. 4*B*. The cell was refractory to a second exposure to PMA.

that most cells that appeared by various criteria to be activated spontaneously early in the experiment (see Methods, Heterogeneous responses to stimulation and possible effects of adherence) responded to PMA after returning to 'normal' behaviour. The multiplicity of events that occur during the first few minutes of an experiment (prodding the cell with the glass pipette tip, applying the $NH_4^+$ gradient to set $pH_i$, and establishing voltage-clamp control during insertion of amphotericin into the membrane) obscures the precise state of the cell at that time. It is conceivable that every cell is 'activated' to some extent, and that most recover spontaneously before we have made the first measurement. In summary, secondary exposure of an eosinophil to PMA produced either no response or a weaker response, suggesting that some step in the PMA response pathway is not completely reversible within the time frame of these experiments.

### Zinc sensitivity

All voltage-gated proton channels are inhibited by $ZnCl_2$ (DeCoursey & Cherny, 1994). $Zn^{2+}$ does not simply block $H^+$ channels; it alters gating, slowing activation profoundly and shifting the voltage dependence of gating toward more positive potentials (Cherny & DeCoursey, 1999). It was reported recently that the $H^+$ currents that are activated in eosinophils under conditions when NADPH oxidase is functioning have a higher $Zn^{2+}$ sensitivity than the $H^+$ channels in unstimulated cells and thus are conducted through a different type of $H^+$ channel (Bánfi *et al.* 1999). Therefore, we examined the effects of $ZnCl_2$ on $H^+$ currents in eosinophils before and after activation with PMA. The effects were qualitatively the same in both conditions. Figure 6 shows $H^+$ currents elicited by identical families of pulses in the same eosinophil in the presence of 1 $\mu$M $ZnCl_2$ (Fig. 6*A*) and after washout with a solution containing EGTA to ensure complete removal of $Zn^{2+}$ (Fig. 6*B*). It is evident that the activation of $H^+$ current was slowed profoundly by $Zn^{2+}$, and that $V_{threshold}$ was shifted toward more positive voltages. The cell was then stimulated with PMA, which produced the usual effects on voltage-gated proton channels and turned on −5 pA of $I_e$. A family of pulses in the presence of 1 $\mu$M $ZnCl_2$ is shown in Fig. 6*C*, and currents during the same family of pulses are shown in Fig. 6*D* after washout with EGTA-containing solution. The effects of $ZnCl_2$ are quite similar before and after PMA stimulation: profound slowing of activation and a shift of $V_{threshold}$ toward more positive voltages. The slowing of activation was so profound that even with longer pulses (16–20 s) in this and other experiments, we could not determine $\tau_{act}$ reliably in the presence of 1 $\mu$M $ZnCl_2$. We estimate that the slowing at a given voltage was at least 8- to 10-fold, both in unstimulated and PMA-activated cells. The shift of the $g_H - V$ relationship averaged 35–40 mV in five unstimulated eosinophils and three PMA-activated eosinophils. With due consideration of the complexity of the effects of $ZnCl_2$ on voltage-gated proton channels, within the resolution of these measurements we could detect no difference in the type or magnitude of the effects of $Zn^{2+}$ on voltage-gated proton channels in unstimulated and PMA-activated eosinophils.

## DISCUSSION

### $H^+$ current properties in eosinophils in the permeabilized patch configuration

Human eosinophils have the highest reported $H^+$ current density of any native cell, up to hundreds of picoamps per picofarad (Gordienko *et al.* 1996; Schrenzel *et al.* 1996). At first glance, the $H^+$ current amplitudes in eosinophils studied here with the permeabilized patch approach appear relatively modest. However, the prodigious $H^+$

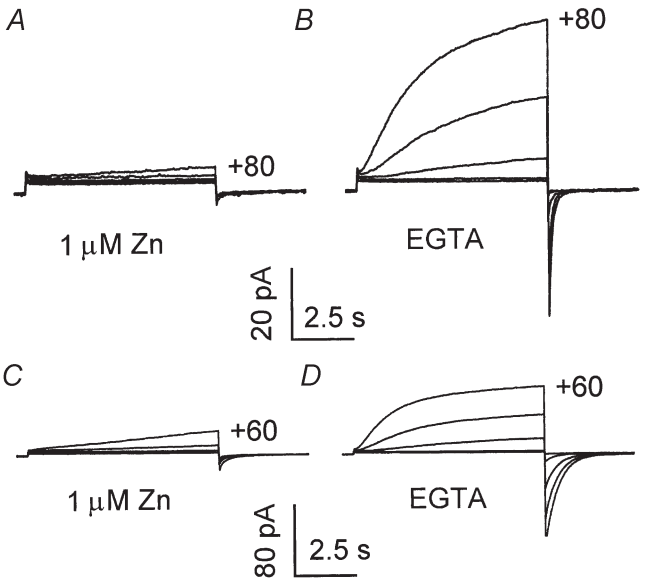


**Figure 6. The $ZnCl_2$ sensitivity of $H^+$ current is the same before and after activation with PMA**

*A*, a family of currents in an unstimulated eosinophil in the presence of 1 $\mu$M $ZnCl_2$ during pulses to 0 mV through +80 mV in 20 mV increments. In contrast with our usual bath solution, this solution had no EGTA. *B*, the same family of pulses applied after complete removal of $ZnCl_2$ by washout with an EGTA-containing solution. The pulses families in *A* and *B* were started 16 and 18 min, respectively, after establishing permeabilized patch recording. The upper calibration bars apply to both *A* and *B*. *C*, approximately 21 min after starting the experiment, PMA was added, and the cell responded in the usual manner: $H^+$ current activation was shifted to a more negative voltage range, $\tau_{tail}$ was characteristically slower, and −5 pA of $I_e$ appeared. After 8 min 1 $\mu$M $ZnCl_2$ was added and the family in *C* was recorded. The currents illustrated are for pulses to −20 mV through +60 mV in 20 mV increments. *D*, the same family of pulses applied after washout of the $Zn^{2+}$. The families in *C* and *D* were started 29 and 32 min after starting the experiment. The lower calibration bars apply to *C* and *D*. The largest tail current in *D* was off-scale and was slightly truncated.

current density in whole-cell studies was observed at low $pH_i$ (Gordienko *et al.* 1996; Schrenzel *et al.* 1996). At $pH_i$ 7.0, the $I_H$ at the end of a 2 s pulse was 25 pA at +80 mV and 54 pA at +100 mV in the whole-cell configuration (Gordienko *et al.* 1996). These amplitudes are similar to the representative data shown in Fig. 1 and to the average $I_H$ at the end of 8 s pulses to +80 mV of 48 pA in untreated eosinophils studied in permeabilized patch configuration. Because we applied longer pulses, we observed more complete activation at each voltage. Thus, there appears to be general agreement between the amplitudes of $H^+$ currents under both sets of recording conditions. Because previous authors did not report gating kinetics in detail, we cannot compare the kinetics described here directly with those in whole-cell studies of eosinophils. Inspection of published whole-cell data (Gordienko *et al.* 1996; Schrenzel *et al.* 1996) suggests that any differences are small.

Like voltage-gated proton currents in other phagocytes (Kapus *et al.* 1993; DeCoursey & Cherny, 1993), those in eosinophils have slow gating kinetics. The conductance activates upon depolarization with $\tau_{act}$ of several seconds. The recording conditions in the present study are reasonably close to being physiological with respect to $pH_o$, $pH_i$, and having intact cytoplasm. The temperature, to which voltage-gated proton channels are extremely sensitive (Kuno *et al.* 1997; DeCoursey & Cherny, 1998), is clearly far from physiological. Correcting $\tau_{act}$ measured at +40 mV in unstimulated eosinophils at 20 °C (Fig. 1*C*) to 37 °C gives ~100 ms, which is a rapid response relative to the ~5 s latency of for $H_2O_2$ generation and the half-time of 2.2 s for arachidonic acid release from guinea-pig eosinophils stimulated with leukotriene $B_4$ (Lindsay *et al.* 1998). Voltage-gated proton channels are thus kinetically competent to be activated as rapidly as the earliest events that occur during a receptor-mediated respiratory burst in eosinophils.

$H^+$ channels in eosinophils were exquisitely sensitive to $Zn^{2+}$. The effects observed in both unstimulated and PMA-activated cells were similar and were qualitatively like those in all voltage-gated proton channels studied to date (DeCoursey & Cherny, 1994; Cherny & DeCoursey, 1999). There is no evidence of significant simple block, in the sense of state-independent channel occlusion. One micromolar $ZnCl_2$ slowed $\tau_{act}$ by roughly an order of magnitude and shifted the $g_H - V$ relationship by 35–40 mV. In the $H^+$ channels of rat alveolar epithelial cells, both of these effects occurred at ~10 $\mu$M $ZnCl_2$ at $pH_o$ 7 (Cherny & DeCoursey, 1999). $H^+$ channels in eosinophils are thus an order of magnitude more sensitive to $Zn^{2+}$. This difference reinforces the idea that the epithelial (type e) channel is a different isoform from the phagocyte (type p) channel (DeCoursey, 1998).

### Electron currents and $O_2^-$ release reflect NADPH oxidase activation by PMA

DPI-sensitive inward currents were activated in most human eosinophils upon the initial application of PMA in permeabilized patch conditions. This inward current is a direct reflection of electron efflux across the membrane through the NADPH oxidase enzyme complex and, thus, referred to as electron current, $I_e$. The following evidence supports this conclusion.

1. The putative $I_e$ is inhibited by DPI.

2. Activation of $I_e$ occurs in permeabilized patch configuration but not whole-cell configuration, which is consistent with it reflecting a diffusible second messenger-mediated response.

3. The kinetics of $I_e$ turn on upon stimulation with PMA are appropriate. The time course was variable, but usually there was a clear delay before the maximal rate of $I_e$ turn on took place. This sigmoidal onset is consistent with the ~1 min delay before the onset of $O_2^-$ release in time-resolved measurements in human eosinophils at 37 °C (Petreccia *et al.* 1987), in human neutrophils at 37 °C (Quinn *et al.* 1993), in pig neutrophils at 22–24 °C (Kapus *et al.* 1992), and in guinea-pig eosinophils at 25 °C (Lacy *et al.* 1999).

4. The amplitude of $I_e$ was three times larger in eosinophils than neutrophils, consistent with $O_2^-$ generation rates reported here (Fig. 3) and in the literature. The peak $I_e$ elicited by PMA was −6.0 pA in eosinophils (Table 1), distinctly larger than −2.3 pA found in neutrophils under similar conditions (DeCoursey *et al.* 2000). The maximum rate of $O_2^-$ release measured in eosinophils and neutrophils was 2.8 and 0.87 nmol $(10^5 \text{ cells})^{-1}$ $(5 \text{ min})^{-1}$, respectively, which can be converted to −9.1 and −2.8 pA of $I_e$. Both results are in excellent agreement with the roughly 3-fold higher $O_2^-$ release in human or guinea-pig eosinophils compared with neutrophils stimulated with PMA or other respiratory burst agonists (DeChatelet *et al.* 1977; Yamashita *et al.* 1985; Shult *et al.* 1985; Petreccia *et al.* 1987; Yagisawa *et al.* 1996; Someya *et al.* 1997).

Electron currents were reported previously in human eosinophils dialysed with an artificial solution containing NADPH and other factors (Schrenzel *et al.* 1998). The peak inward current was −15.6 pA with NADPH in the pipette and −7 pA without NADPH (Schrenzel *et al.* 1998). The former value is somewhat higher than the present results, but the relevant comparison may be with cells without added NADPH, as our experimental procedure provided no external source of NADPH.

An $I_e$ of −6 pA reflects efflux of $3.75 \times 10^7$ electrons $s^{-1}$ $cell^{-1}$. Given an estimate of the total number of functioning NADPH oxidase complexes in each cell, we can calculate the turnover rate of the enzyme. In human neutrophils ~250 000 molecules each of $p47^{phox}$, $p67^{phox}$, and *rac* are translocated to the membrane within 6 min of PMA stimulation (Quinn *et al.* 1993). It appears that continuous translocation of these components is required for sustained $O_2^-$ release. If we nevertheless assume that all 250 000 molecules form simultaneously active NADPH

oxidase complexes, and scale this number up by a factor of 2–3 to reflect the proportionately higher content of NADPH oxidase components in eosinophils (Segal *et al.* 1981; Yagisawa *et al.* 1996; Someya *et al.* 1997), then each enzyme complex pumps 300–450 electrons $s^{-1}$ out of the cell. This estimate is in good agreement with the turnover rate of NADPH oxidase in a cell-free system of 240–330 $s^{-1}$ (Koshkin *et al.* 1997; Cross *et al.* 1999). This order of magnitude agreement either confirms the estimate of the number of active NADPH oxidase complexes in each eosinophil or it validates the estimate of the turnover rate of the enzyme, depending on which value one finds more reliable.

### Comparison of PMA response of $H^+$ channels with that of neutrophils

The responses of eosinophils to PMA described here are qualitatively similar to those of neutrophils (DeCoursey *et al.* 2000). In response to PMA, $H^+$ currents activate faster (smaller $\tau_{act}$), the maximum $H^+$ conductance increases, tail current decay is slowed dramatically, and the $g_H$–$V$ relationship is shifted about 40 mV more negative. There were several quantitative differences between the responses of eosinophils and neutrophils. The PMA-induced changes in $H^+$ currents were generally slightly faster in eosinophils (Table 1). Significantly, the responses in eosinophils were more transient, with the $I_e$ as well as the $H^+$ current parameters often reversing spontaneously, at least partially, within 10–20 min after addition of PMA. In neutrophils, partial spontaneous reversal of the activation of $I_e$ and the slowing of $\tau_{tail}$ in response to PMA occurred infrequently. A more pronounced difference is that in neutrophils we never observed convincing reversal of the PMA-induced increase in $I_H$, the more rapid activation rate, or the hyperpolarizing shift of the $g_H$–$V$ relationship. In contrast, in many eosinophils all of these parameters reversed spontaneously over time. In both neutrophils and eosinophils in which $I_e$ turned off spontaneously, the PMA-induced slowing of $\tau_{tail}$ usually reversed in parallel. It is possible that the PMA enhancement of $I_H$ might have reversed eventually in neutrophils, but we saw no evidence of this in some experiments lasting 1 h or more (DeCoursey *et al.* 2000). The transience of $I_e$ in eosinophils compared with neutrophils is consistent with the more transient time course of PMA-stimulated $O_2^-$ generation in eosinophils observed here (Fig. 3) and in previous studies (Shult *et al.* 1985).

All of the changes in $H^+$ channels that occur upon PMA stimulation are in the direction expected to result from cytoplasmic acidification. Because NADPH oxidase activity itself generates intracellular protons, it is reasonable to ask to what extent the changes might be the result of a decrease in $pH_i$ rather than modulation of the properties of voltage-gated proton channels. Indeed, $V_{rev}$ was more negative after PMA treatment indicating that slight cytoplasmic acidification did occur in spite of the $NH_4^+$ gradient. The actual change in $pH_i$ depends on the balance between two opposing forces. Because there is a direct proportionality between electron translocation across the membrane and protons deposited into the cell by NADPH oxidase, it can be considered that $I_e$ directly indicates the acid load on the cell. Thus $I_e$ of −6 pA reflects a requisite continuous net cytoplasmic acidification equivalent to −6 pA of $H^+$ current (i.e. influx of $3.75 \times 10^7$ $H^+$ $s^{-1}$ $cell^{-1}$). Opposing this acid load is the applied $NH_4^+$ gradient, whose ability to clamp $pH_i$ will be influenced by cell size and pipette geometry. After treatment of eosinophils with PMA, $V_{rev}$ shifted on average −5.8 mV, corresponding to a decrease in $pH_i$ of ~0.1 unit. Because DPI partially reversed the shift, at least part of the $pH_i$ shift is attributable to NADPH oxidase-induced acidification. A drop in $pH_i$ of 0.1 units will shift the $g_H$–$V$ relationship only −4 mV according to the empirical observation that over a wide range the $g_H$–$V$ relationship changes by 40 mV per unit change in $\Delta pH$ (Cherny *et al.* 1995). Thus, at most 10 % of the $g_H$–$V$ shift is ascribable to the lower $pH_i$. The slowing of $\tau_{tail}$ and speeding of $\tau_{act}$ predicted to occur due to a 0.1 unit drop in $pH_i$ based on the slopes in Fig. 1*C* and assuming a −4 mV shift of all kinetic parameters would be 14 and 6 %, respectively. The peak changes in $\tau_{tail}$ and $\tau_{act}$ produced by PMA were 540 and 417 %, respectively (Table 1). Thus, only a tiny fraction of the changes in $H^+$ channel gating kinetics can be ascribed to a loss of control over $pH_i$ due to the functioning of NADPH oxidase or other causes. PMA must modulate the properties of $H^+$ channels themselves, rather than changing their microenvironment.

### Does PMA activate a new type of $H^+$ channel or modulate existing channels?

Human eosinophils studied in conventional whole-cell configuration express very large voltage-gated proton currents with properties similar to those in other phagocytes (Gordienko *et al.* 1996; Schrenzel *et al.* 1996). However, in human eosinophils studied in whole-cell configuration with NADPH and other factors included in the pipette to elicit NADPH oxidase function, the properties of voltage-gated proton channels were markedly different (Bánfi *et al.* 1999). The $g_H$ activated in a much more negative voltage range, with the result that inward $H^+$ currents were activated negative to $E_H$ at some pH. In addition, $\tau_{tail}$ was quite slow. Bánfi *et al.* (1999) hypothesized that a novel type of voltage-gated proton channel was activated when the NADPH oxidase was working. This $H^+$ channel (type x) was postulated to be distinct from the type p $H^+$ channels observed in conventional whole-cell technique. In unstimulated eosinophils in permeabilized patch configuration proton currents exhibit type p properties like those in whole-cell studies (Gordienko *et al.* 1996; Schrenzel *et al.* 1996). After PMA activation the $H^+$ currents exhibit clear type x properties, including activation of inward currents and very slow $\tau_{tail}$.

In neutrophils, we concluded that a single population of $H^+$ channels was present and that PMA greatly alters the properties of these channels but does not induce a new type of channel (DeCoursey *et al.* 2000). The $g_H$ increased in direct proportion to the resting $g_H$, consistent with modulation rather than induction of an independent conductance. Tail current decay was monoexponential before, during and after the slowing by PMA both in neutrophils and in many eosinophils. Similarly, the $g_H-V$ relationship did not exhibit evidence of two components. The strongest evidence for the existence of two distinct types of channels was that type x currents seemed to be 20-fold more sensitive to $Zn^{2+}$ inhibition than type p currents (Bánfi *et al.* 1999). In contrast, in the present study, the inhibition of $H^+$ currents by $Zn^{2+}$ in human eosinophils was similar in unstimulated and PMA-activated cells. In the Appendix, we show that the apparent differences between our conclusions and those of Bánfi *et al.* (1999) reflect differences in the way that $Zn^{2+}$ effects were assessed. The similarity of $Zn^{2+}$ sensitivity of $H^+$ currents in eosinophils before and after PMA activation provides further support for the idea that a single population of $H^+$ channels exists. PMA strongly modulates the properties of these channels, greatly enhancing their probability of opening.

## APPENDIX

We interpret the effects of PMA on proton channels in human eosinophils as modulation of the properties of channels that are present in the surface membrane of resting cells. In the present study, we see evidence of only one population of channels, and by our criteria, the $Zn^{2+}$ sensitivity was the same in unstimulated and PMA-activated eosinophils. In contrast, Bánfi *et al.* (1999) proposed that eosinophils express two distinct varieties of voltage-gated proton channels. A 'high-threshold' channel that opens at voltages positive to $E_H$ is present in the surface membrane of unstimulated cells. A 'low-threshold' channel is absent from resting cells but appears when NADPH oxidase is active. This channel is unique among $H^+$ channels in activating negative to $E_H$ under some conditions, resulting in inward current. The 'low-threshold' channel was reported to be 20-fold more sensitive to inhibition by $Zn^{2+}$ (Bánfi *et al.* 1999). This conclusion was based on comparison of concentration–response relations at two voltages: at +20 mV where (under their conditions) there was inward $H^+$ current attributed to the 'low-threshold' conductance, and at +60 mV where 'high-threshold' channels would also be activated. The concentration–response curve was shifted toward higher $[Zn^{2+}]$ at the more positive test voltage. In this Appendix we show that these results are qualitatively consistent with the existence of a single population of voltage-gated proton channels. In fact, the apparent $Zn^{2+}$ potency as measured by Bánfi *et al.* (1999) *must* depend on test potential to the extent that its effects are due to its ability to shift the voltage dependence of $H^+$ channel gating.

$Zn^{2+}$ and other divalent metals have several effects on all voltage-gated proton channels that have been studied, and have similar effects on many other types of ion channels. The voltage–activation curve is shifted to more positive voltages, the activation of current during a depolarizing pulse is slowed, and maximal $g_H$ may be decreased. We report here that $Zn^{2+}$ exhibits these effects, in particular the depolarizing voltage shift, in human eosinophils both before and after activation by PMA. It is not easy to distinguish among these effects; some slowing of $\tau_{act}$ is expected from the voltage shift of gating. For the present purpose, we test the simple assumption that the entire effect of $Zn^{2+}$ is due to its voltage-shifting ability, which results from $Zn^{2+}$ binding to a site at the external side of the channel (Cherny & DeCoursey, 1999) with affinity $K_M = 10^{-7}$ M (set arbitrarily for the purpose of illustration). We describe the $g_H-V$ relationship in the absence of $Zn^{2+}$ as a Boltzmann distribution with midpoint at 0 mV and a slope factor of 10 mV. As discussed previously (p. 832 of Cherny & DeCoursey, 1999), given simple assumptions, the voltage shift actually produced by $Zn^{2+}$ can be described empirically from the slope factor of the $g_H-V$ relationship and the $K_M$ of $Zn^{2+}$. Figure 7*A* shows the predicted voltage shift as a function of $Zn^{2+}$ concentration; the inset illustrates a voltage shift at one arbitrary concentration of $Zn^{2+}$.

Ion channel block is often quantified as the ratio of the current in the presence of blocker to that in its absence. This procedure was used by Bánfi *et al.* (1999). The implicit assumption is that the blocker simply occludes the channel, with no dependence on voltage or the gating state of the channel, and conversely, the blocker does not alter the gating kinetics or voltage dependence of the channel. It is abundantly clear that $Zn^{2+}$ has profound effects on both the gating kinetics and voltage dependence of voltage-gated proton channels (Cherny & DeCoursey, 1999). In fact, 'block' in the sense of simple channel occlusion is at most a minor part of the actions of $Zn^{2+}$. The inset in Fig. 7*A* illustrates how a simple voltage shift affects the current measured at different voltages, V1 and V2. The fractional decrease in $H^+$ current measured at the end of the pulse is much greater at test voltage V1, as can also be seen from the intersection of the lines in the schematic $g_H-V$ relationships. Thus, the apparent affinity of $Zn^{2+}$ for the $H^+$ channel will depend on the test voltage.

Figure 7*B* illustrates the calculated concentration–response relationships that result when $Zn^{2+}$ effects are evaluated as the ratio of current in the presence and absence of $Zn^{2+}$. The curves calculated for different test voltages resemble experimental data that were analysed in this way (Bernheim *et al.* 1993; Gordienko *et al.* 1996;

Bánfi *et al.* 1999). Except at negative voltages where the open probability of the channel is very low, the apparent potency of $Zn^{2+}$ is strongly dependent on the test voltage, with the calculated apparent $K_i$ increasing about 20-fold for a test voltage 40 mV more positive. Bánfi *et al.* (1999) reported that the $K_i$ of $Zn^{2+}$ was 20-fold higher when the test voltage was +60 mV compared with +20 mV. Thus, rather than comprising evidence of two types of channels, the $Zn^{2+}$ concentration–response data of Bánfi *et al.* (1999) are entirely consistent with the existence of a single population of proton channels.

The dependence of the reduction of $H^+$ current by $Zn^{2+}$ on test voltage gives the impression that 'block' is voltage dependent. However, genuine voltage-dependent block differs in two significant ways from the phenomenon in Fig. 7*B*. First, voltage-dependent block suggests that $Zn^{2+}$ acts at a site within the membrane potential field. There is no evidence that external $Zn^{2+}$ receptor of voltage-gated proton channels is within the membrane potential field, as discussed at length elsewhere (Cherny & DeCoursey, 1999). If the conduction pathway through voltage-gated proton channels is a hydrogen-bonded chain including side groups of amino acids, as has been suspected for some time (DeCoursey & Cherny, 1994), then $Zn^{2+}$ could not permeate. Second, voltage-dependent block implies that the time $Zn^{2+}$ occupies its receptor

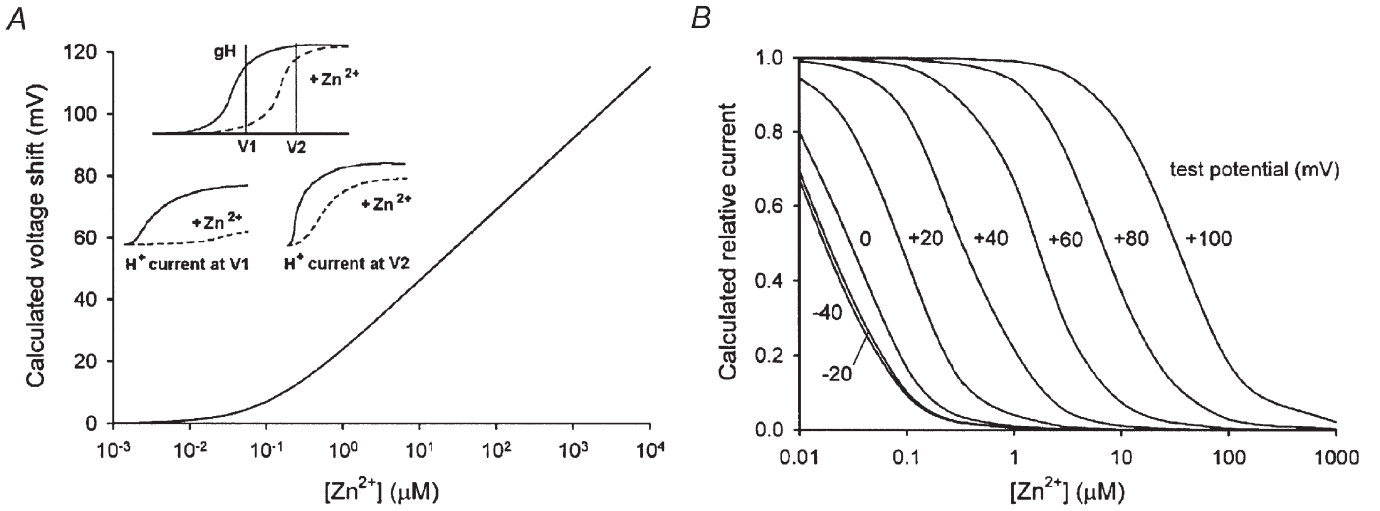


**Figure 7. The depolarizing shift of voltage-dependent gating by $ZnCl_2$ results in test-pulse dependence of apparent $Zn^{2+}$ sensitivity**

*A*, the dependence of the voltage shift of the $g_H$–$V$ relationship on $ZnCl_2$ concentration is illustrated for a semi-empirical model of $Zn^{2+}$ effects on voltage-gated proton channels (Cherny & DeCoursey, 1999). The numerical value of the shift was derived by assuming that the channel cannot open while $Zn^{2+}$ is bound to it. The open probability of the channel in the absence of $Zn^{2+}$ is given by a simple Boltzmann relationship: $P_{open} = (1 + \exp((V - V_{1/2})/k))^{-1}$ where the mid-point potential $V_{1/2}$ was set arbitrarily at 0 mV and the slope factor $k$ is −10 mV, a value typical for voltage-gated proton channels in many cells (DeCoursey & Cherny, 1994). By definition, if $k = -10$ mV then $P_{open}$ is reduced e-fold in 10 mV. Hence, if $Zn^{2+}$ reduced $P_{open}$ e-fold this would shift the $g_H$–$V$ relationship by 10 mV (Cherny & DeCoursey, 1999). The curve is drawn according to: $V_{shift} = \ln(1 - P_{Zn})^{-1} \times 10$ mV, where $V_{shift}$ is the voltage shift in mV, and $P_{Zn}$ is the probability that the channel has $Zn^{2+}$ bound. In turn, $P_{Zn}$ is given by: $P_{Zn} = (1 + [K_M]/[Zn^{2+}])^{-1}$ which assumes simple first-order binding with a binding constant $K_M = 10^{-7}$ M. Whether or not the assumptions underlying the relationship in *A* are valid, the experimentally observed $[Zn^{2+}]$ dependence of the voltage shift is approximated well by this model (Cherny & DeCoursey, 1999). The inset illustrates the effect of a simple voltage shift. The upper diagram shows a right shift in the $g_H$–$V$ relationship produced by $Zn^{2+}$ (dashed lines). The lower diagrams illustrate the appearance of currents measured at two voltages, V1 and V2, in the absence (continuous curves) or presence (dashed curves) of $Zn^{2+}$. *B*, apparent concentration–response curves calculated on the assumption that the entire effect of $Zn^{2+}$ can be described as a voltage shift. The relative current measured during a given voltage pulse will be reduced simply because $P_{open}$ is reduced at each voltage when the $g_H$–$V$ relationship is shifted toward more positive voltages. The ratio plotted is of $P_{open}$ after the voltage shift derived from *A* for each concentration of $Zn^{2+}$ normalized to $P_{open}$ in the absence of $Zn^{2+}$. This corresponds with an idealized current ratio. Real current data would generally be complicated by the fact that the currents do not reach steady state with pulse durations normally employed, and the profound slowing effect of $Zn^{2+}$ exacerbates this problem. The concentration–response relationships plotted here are somewhat steeper than a normal dose–response curve in which there is 1:1 binding of drug to a receptor.

depends on voltage. There is no evidence that this is the case, and Fig. 7*B* illustrates that existing data are well described by assuming that $Zn^{2+}$ occupies its receptor independently of membrane potential.


Babior, B. M. (1999). NADPH oxidase: an update. *Blood* **93**, 1464–1476.

Bánfi, B., Schrenzel, J., Nüsse, O., Lew, D. P., Ligeti, E., Krause, K.-H. & Demaurex, N. (1999). A novel $H^+$ conductance in eosinophils: unique characteristics and absence in chronic granulomatous disease. *Journal of Experimental Medicine* **190**, 183–194.

Bernheim, L., Krause, R. M., Baroffio, A., Hamann, M., Kaelin, A. & Bader, C.-R. (1993). A voltage-dependent proton current in cultured human skeletal muscle myotubes. *Journal of Physiology* **470**, 313–333.

Cherny, V. V., DeCoursey, A. G., Henderson, L. M., Thomas, L. L. & DeCoursey, T. E. (2001*a*). Proton and electron currents during the respiratory burst in human eosinophils. *Biophysical Journal* **80**, 506–507a (abstract).

Cherny, V. V. & DeCoursey, T. E. (1999). pH dependent inhibition of voltage-gated $H^+$ currents in rat alveolar epithelial cells by $Zn^{2+}$ and other divalent cations. *Journal of General Physiology* **114**, 819–838.

Cherny, V. V., Henderson, L. M., Xu, W., Thomas, L. L. & DeCoursey, T. E. (2001*b*). Activation of NADPH oxidase-related proton and electron currents in human eosinophils by arachidonic acid. *Journal of Physiology* 535, 783–794.

Cherny, V. V., Markin, V. S. & DeCoursey, T. E. (1995). The voltage-activated hydrogen ion conductance in rat alveolar epithelial cells is determined by the pH gradient. *Journal of General Physiology* **105**, 861–896.

Cross, A. R., Erickson, R. W., Ellis, B. A. & Curnutte, J. T. (1999). Spontaneous activation of NADPH oxidase in a cell-free system: unexpected multiple effects of magnesium ion concentrations. *Biochemical Journal* **338**, 229–233.

Dechatelet, L. R., Shirley, P. S., McPhail, L. C., Huntley, C. C., Muss, H. B. & Bass, D. A. (1977). Oxidative metabolism of the human eosinophil. *Blood* **50**, 525–535.

DeCoursey, T. E. (1998). Four varieties of voltage-gated proton channels. *Frontiers in Bioscience* **3**, d477–482.

DeCoursey, T. E. & Cherny, V. V. (1993). Potential, pH and arachidonate gate hydrogen ion currents in human neutrophils. *Biophysical Journal* **65**, 1590–1598.

DeCoursey, T. E. & Cherny, V. V. (1994). Voltage-activated hydrogen ion currents. *Journal of Membrane Biology* **141**, 203–223.

DeCoursey, T. E. & Cherny, V. V. (1995). Voltage-activated proton currents in membrane patches of rat alveolar epithelial cells. *Journal of Physiology* **489**, 299–307.

DeCoursey, T. E. & Cherny, V. V. (1998). Temperature dependence of voltage-gated $H^+$ currents in human neutrophils, rat alveolar epithelial cells, and mammalian phagocytes. *Journal of General Physiology* **112**, 503–522.

DeCoursey, T. E., Cherny, V. V., Zhou, W. & Thomas, L. L. (2000). Simultaneous activation of NADPH oxidase-related proton and electron currents in human neutrophils. *Proceedings of the National Academy of Sciences of the USA* **97**, 6885–6889.

DeCoursey, T. E. & Grinstein, S. (1999). Ion channels and carriers in leukocytes. In *Inflammation: Basic Principles and Clinical Correlates*, 3rd edn, ed. Gallin, J. I. & Snyderman, R., pp. 639–659. Lippincott Williams & Wilkins, Philadelphia, PA, USA.

Eder, C. & DeCoursey, T. E. (2001). Voltage-gated proton channels in microglia. *Progress in Neurobiology* **64**, 277–305.

Freiburghaus, J., Jörg, A. & Müller, T. (1991). Luminol-dependent chemiluminescence in bovine eosinophils and neutrophils: differential increase of intracellular and extracellular chemiluminescence induced by soluble stimulants. *Journal of Bioluminescence and Chemiluminescence* **6**, 115–121.

Giembycz, M. A. & Lindsay, M. A. (1999). Pharmacology of the eosinophil. *Pharmacological Reviews* **51**, 213–339.

Gleich, G. J. (2000). Mechanisms of eosinophil-associated inflammation. *Journal of Allergy and Clinical Immunology* **105**, 651–663.

Gordienko, D. V., Tare, M., Parveen, S., Fenech, C. J., Robinson, C. & Bolton, T. B. (1996). Voltage-activated proton current in eosinophils from human blood. *Journal of Physiology* **496**, 299–316.

Grinstein, S., Romanek, R. & Rotstein, O. D. (1994). Method for manipulation of cytosolic pH in cells clamped in the whole cell or perforated-patch configurations. *American Journal of Physiology* **267**, C1152–1159.

Hansel, T. T., De Vries, I. J. M., Iff, T., Rihs, S., Wandzilak, M., Betz, S., Blaser, K. & Walker, C. (1991). An improved immunomagnetic procedure for the isolation of highly purified human blood eosinophils. *Journal of Immunological Methods* **145**, 105–110.

Haskell, M. D., Moy, J. N., Gleich, G. J. & Thomas, L. L. (1995). Analysis of signaling events associated with activation of neutrophil superoxide anion production by eosinophil granule major basic protein. *Blood* **86**, 4627–4637.

Henderson, L. M. & Chappell, J. B. (1996). NADPH oxidase of neutrophils. *Biochimica et Biophysica Acta* **1273**, 87–107.

Henderson, L. M., Chappell, J. B. & Jones, O. T. G. (1987). The superoxide-generating NADPH oxidase of human neutrophils is electrogenic and associated with an $H^+$ channel. *Biochemical Journal* **246**, 325–329.

Henderson, L. M., Chappell, J. B. & Jones, O. T. G. (1988*a*). Internal pH changes associated with the activity of NADPH oxidase of human neutrophils, further evidence for the presence of an $H^+$ conducting channel. *Biochemical Journal* **251**, 563–567.

Henderson, L. M., Chappell, J. B. & Jones, O. T. G. (1988*b*). Superoxide generation by the electrogenic NADPH oxidase of human neutrophils is limited by the movement of a compensating charge. *Biochemical Journal* **255**, 285–290.

Horie, S. & Kita, H. (1994). CD11b/CD18 (Mac-1) is required for degranulation of human eosinophils induced by human recombinant granulocyte-macrophage colony-stimulating factor and platelet-activating factor. *Journal of Immunology* **152**, 5457–467.

Kapus, A., Romanek, R., Qu, A. Y., Rotstein, O. D. & Grinstein, S. (1993). A pH-sensitive and voltage-dependent proton conductance in the plasma membrane of macrophages. *Journal of General Physiology* **102**, 729–760.

Kapus, A., Szászi, K. & Ligeti, E. (1992). Phorbol 12-myristate 13-acetate activates an electrogenic $H^+$-conducting pathway in the membrane of neutrophils. *Biochemical Journal* **281**, 697–701.

Koshkin, V., Lotan, O. & Pick, E. (1997). Electron transfer in the superoxide-generating NADPH oxidase complex reconstituted in vitro. *Biochimica et Biophysica Acta* **1319**, 139–146.

Kuno, M., Kawawaki, J. & Nakamura, F. (1997). A highly temperature-sensitive proton conductance in mouse bone marrow-derived mast cells. *Journal of General Physiology* **109**, 731–740.

Lacy, P., Mahmudi-Azer, S., Bablitz, B., Gilchrist, M., Fitzharris, P., Cheng, D., Man, S. F. P., Bokoch, G. M. & MoQbel, R. (1999). Expression and translocation of Rac2 in eosinophils during superoxide generation. *Immunology* **98**, 244–252.

Lindsay, M. A., Perkins, R. S., Barnes, P. J. & Giembycz, M. A. (1998). Leukotriene $B_4$ activates the NADPH oxidase in eosinophils by a pertussis toxin-sensitive mechanism that is largely independent of arachidonic acid mobilization. *Journal of Immunology* **160**, 4526–4534.

Nanda, A. & Grinstein, S. (1991). Protein kinase C activates an $H^+$ (equivalent) conductance in the plasma membrane of human neutrophils. *Proceedings of the National Academy of Sciences of the USA* **88**, 10816–10820.

Petreccia, D. C., Nauseef, W. M. & Clark, R. A. (1987). Respiratory burst of normal human eosinophils. *Journal of Leukocyte Biology* **41**, 283–288.

Quinn, M. T., Evans, T., Loetterle, L. R., Jesaitis, A. J. & Bokoch, G. M. (1993). Translocation of Rac correlates with NADPH oxidase activation: evidence for equimolar translocation of oxidase components. *Journal of Biological Chemistry* **268**, 20983–20987.

Robertson, A. K., Cross, A. R., Jones, O. T. G. & Andrew, P. W. (1990). The use of diphenylene iodinium, an inhibitor of NADPH oxidase, to investigate the antimicrobial action of human monocyte derived macrophages. *Journal of Immunological Methods* **133**, 175–179.

Rothenberg, M. E. (1998). Eosinophilia. *New England Journal of Medicine* **338**, 1592–1600.

Schrenzel, J., Lew, D. P. & Krause, K.-H. (1996). Proton currents in human eosinophils. *American Journal of Physiology* **271**, C1861–1871.

Schrenzel, J., Serrander, L., Bánfi, B., Nüsse, O., Fouyouzi, R., Lew, D. P., Demaurex, N. & Krause, K.-H. (1998). Electron currents generated by the human phagocyte NADPH oxidase. *Nature* **392**, 734–737.

Segal, A. W., Garcia, R., Goldstone, A. H., Cross, A. R. & Jones, O. T. G. (1981). Cytochrome $b_{245}$ of neutrophils is also present in human monocytes, macrophages and eosinophils. *Biochemical Journal* **196**, 363–367.

Shult, P. A., Graziano, F. M., Wallow I. H. & Busse, W. W. (1985). Comparison of superoxide generation and luminol-dependent chemiluminescence with eosinophils and neutrophils from normal individuals. *Journal of Laboratory and Clinical Medicine* **106**, 638–645.

Someya, A., Nishijima, K., Nunoi, H., Irie, S. & Nagaoka, I. (1997). Study on the superoxide-producing enzyme of eosinophils and neutrophils—comparison of the NADPH oxidase components. *Archives of Biochemistry and Biophysics* **345**, 207–213.

Wu, W., Samoszuk, M. K., Comhair, S. A. A., Thomassen, M. J., Farver, C. F., Dweik, R. A., Kavuru, M. S., Erzurum, S. C. & Hazen, S. L. (2000). Eosinophils generate brominating oxidants in allergen-induced asthma. *Journal of Clinical Investigation* **105**, 1455–1463.

Yagisawa, M., Yuo, A., Yonemaru, M., Imajoh-Ohmi, S., Kanegasaki, S., Yazaki, Y. & Takaku, F. (1996). Superoxide release and NADPH oxidase components in mature human phagocytes: correlation between functional capacity and amount of functional proteins. *Biochemical and Biophysical Research Communications* **228**, 510–516.

Yamashita, T., Someya, A. & Hara, E. (1985). Response of superoxide anion production by guinea pig eosinophils to various soluble stimuli: comparison to neutrophils. *Archives of Biochemistry and Biophysics* **241**, 447–452.

**Acknowledgements**

Supported by the National Heart, Lung, and Blood Institute of the National Institutes of Health (grants HL52671 and HL61437 to T.D.) and by the National Institute of Allergy and Infectious Diseases of the National Institutes of Health (grant AI48160 to L.T.). The authors appreciate the able technical assistance of Tatiana Iastrebova.

**Corresponding author**

T. E. DeCoursey: Department of Molecular Biophysics and Physiology, Rush Presbyterian St. Luke's Medical Center, 1653 West Congress Parkway, Chicago, IL 60612, USA.

Email: tdecours@rush.edu